Chapter 1

Introduction

This thesis deals with the structure of the ripple ($P_{\beta'}$) phase of phospholipids. In this chapter we give a brief introduction to this phase. Section-1.1 is devoted to general properties of lipids and surfactants and to the phase behavior of phospholipids. In section-1.2 previous work on the ripple phase is discussed with special emphasis on freeze fracture and x-ray studies.

1.1 Phospholipids: structure and phase behavior

Lipids are defined not by their molecular structure but by their solubility [1]. Biochemical substances that are soluble in non-polar organic solvents are called lipids and include triglycerides, steroids, phospholipids, waxes and so on. Mixtures of various lipids and proteins constitute the cell membrane and membranous organelles of all living cells.

Phospholipids are amphiphilic molecules with a polar hydrophilic (water loving) group and one or more hydrophobic (water hating) hydrocarbon chains. The hydrophilic group is referred to as the head-group and the chains are referred to as tails. Phospholipids are so called because of the presence of a phosphorus atom in the head-group. Phospholipids have a glycerol backbone with the phosphate in the 3-position (see figure-1.1). There are usually two hydrocarbon chains at 1 and 2 positions of the backbone, that constitute the hydrophobic tail. The chains are joined to the backbone through either an ether or an ester linkage. Most naturally occur-

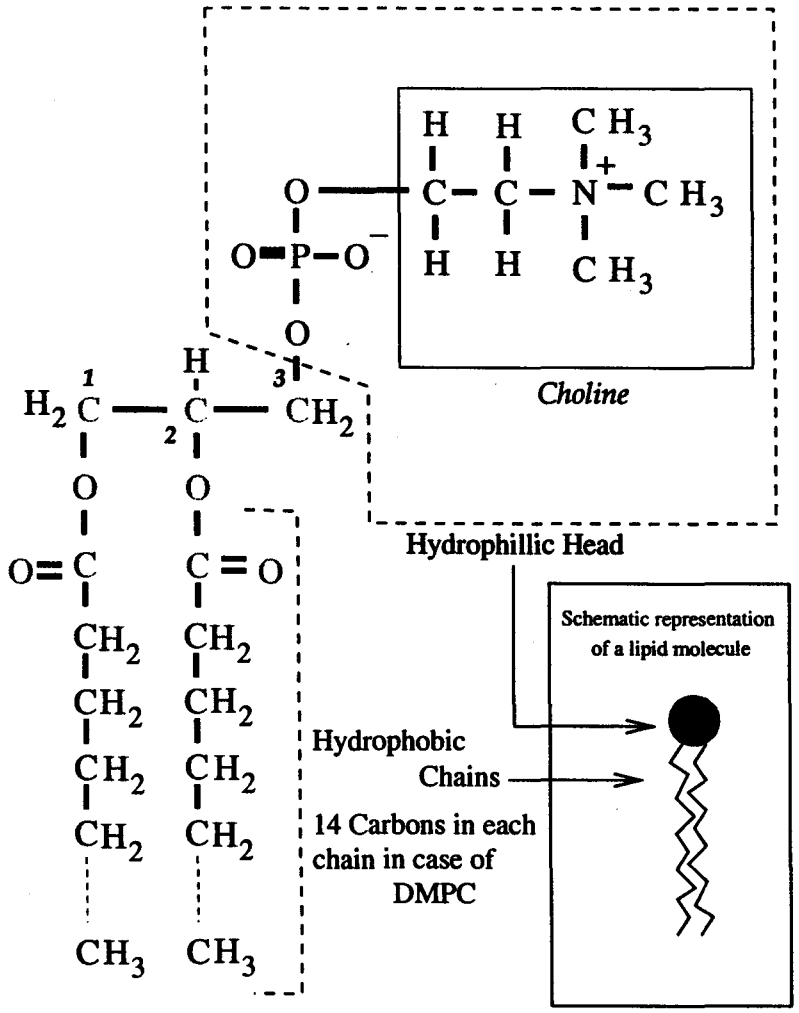

Figure 1.1: **Schematic diagram of the structure of 1,2 dimyristoyl 3 phosphatidylcholine (DMPC).**

ring phospholipids have two chains, but one chain derivatives are also known. These one chain derivatives tend to be water soluble, whereas the two chain phospholipids are generally insoluble in water though they can incorporate some amount of water and swell to a certain extent. The hydrocarbon chain(s) can be either saturated or can have one or more double bonds. In case of the double chained lipids, the two chains may or may not be similar. The two chains can vary both in the number of carbon atoms and in the number of double bonds present. The head-group is usually either zwitter-ionic or charged and this gives rise to strong attractive (hydrophilic) interaction between the head-group and water. The charge of the head-group can be affected by the pH of the environment.

Table 1.1: Structure and nomenclature of Lipids that are referred to in this chapter. C^1 and C^2 are the number of carbon atoms in the chains at position 1 and 2 respectively. db is the number of double bonds.

Full name	abbreviation	C^1	C^2	db	linkage
Dipalmitoylphosphatidylcholine	DPPC	16	16	0	ester
Dimyristoylphosphatidylcholine	DMPC	14	14	0	ester
Dilauroylphosphatidylcholine	DLPC	12	12	0	ester
Dihexadecyl phosphatidylcholine	DHPC	16	16	0	ether
Palmitoyl-oleoyl phosphatidylcholine	POPC	18	16	1	ester
Dipalmitoylphosphatidylethanolamine	DPPE	16	16	0	ester

Phosphatidylcholines (also called lecithins) are one of the most studied class of lipids and form the subject of this thesis. In phosphatidylcholines, a choline moiety (figure-1.1) is attached to the phosphate in the head-group. The choline has a nitrogen with three methyl groups attached to it. This makes the phosphatidylcholine head-group rather bulky. Phosphatidylcholines are zwitter-ionic at neutral pH: in water, the nitrogen acquires a positive charge and the phosphate acquires a negative charge. The phosphatidylethanolamine head-group is similar except that the $(CH)_3$ groups attached to the nitrogen are replaced by hydrogen atoms. A list of various lipids that are referred to in this thesis, along with their structures, is give in table-1.1.

1.1.1 The hydrophobic effect

The strong inclination of water molecules to form hydrogen bonds with each other influences their interactions with non-polar molecules that are incapable of forming hydrogen bonds. Hydrocarbons are examples of such non-polar or inert moieties. When water molecules come in contact with such non-polar molecules, in order to maximize the number of hydrogen bonds between themselves, the water molecules have to get rearranged around the inert molecules. But this process involves disruption of existing water structure and imposition of a new and more ordered structure around the non-polar molecules. This reduces the entropy of the system and is therefore thermodynamically unfavorable. This is the reason why hydrocarbon chains are insoluble in water (hydrophobic) [2].

1.1.2 Self-assembly of amphiphilic molecules

When amphiphilic molecules are dissolved in water, they form various structures such that the hydrophilic parts are in contact with water whereas the hydrophobic parts are shielded from water [2]. Figure-1.2 shows a few such possible structures. At very low concentrations, a monolayer is formed at the air-water interface such that the head-groups are in contact with water and the chains face the air. This sort of arrangement of the amphiphilic molecules reduces the surface tension and therefore such molecules are called surface active agents or surfactants. At low concentrations, all the molecules in the bulk are dispersed as single molecules (monomers). As more surfactants are added to the system, the monomer concentration increases till at a critical concentration (called the critical micellar concentration or CMC), they start forming aggregates (called micelles). If even more surfactants are added, the new molecules go into aggregates and the monomer concentration remains at CMC. Just above CMC, the micelles are usually spherical. They may become rod-like or disc-like at higher concentrations. Anisotropic micelles (rods and discs) can form orientationally ordered nematic liquid crystalline phases at high concentrations. At even higher concentrations, the rod-like cylindrical micelles can become very long and form a hexagonal phase, where the long cylinders are arranged on a two-dimensional hexagonal lattice. Similarly, the radius of disc-like micelles can become very large at high surfactant concentrations and this leads to the formation of a lamellar phase. Lipids in water form such layered structures where water layers are separated by two molecules thick lipid bilayers (figure-1.2). The bilayers can curve back on themselves to form closed bag like structures called vesicles (figure-1.2). These vesicles can be unilamellar (made of single bilayer) or multilamellar (many bilayers) though there is some evidence to indicate that the unilamellar structures are not equilibrium structures [3]. Depending upon the temperature and humidity, the lipid bilayers exhibit many different phases which are discussed later in this chapter.

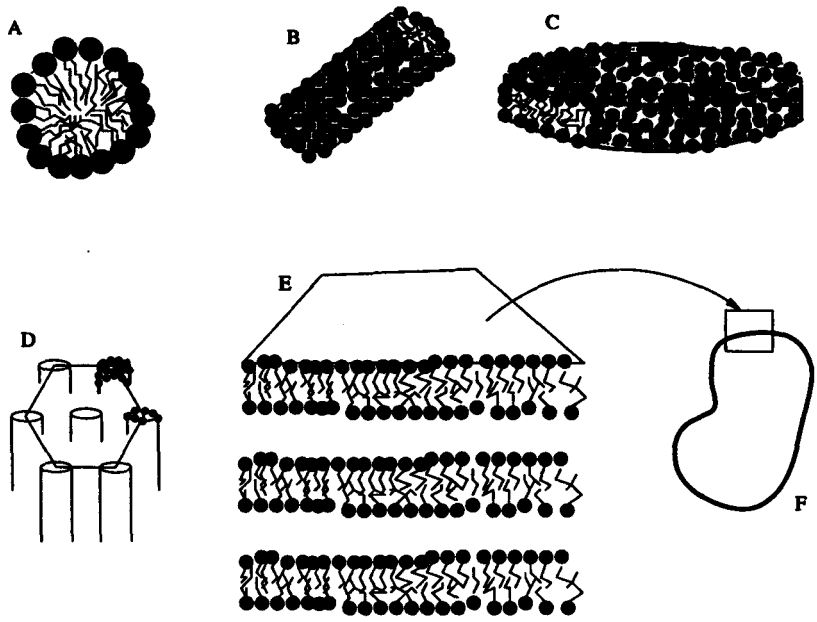

Figure 1.2: **Schematic diagram of some structures formed by amphiphilic molecules in water. A: Spherical micelle, B:cylindrical micelle, C: disc-like micelle, D: hexagonal phase, E: Bilayers in lamellar phase, F: bilayers folding up to form a vesicle.**

1.1.3 Phase diagram of hydrated phospholipids

The phases exhibited by lipids depend on the temperature and the water content. Dry lecithin has a crystalline phase at low temperatures. It undergoes a chain melting transition at about 110°C above which it exhibits various liquid crystalline phases or mesophases, characterized by some partial ordering of the molecules [3]. Above about 250°C, an isotropic liquid is formed. Anhydrous lecithins are difficult to obtain and hence most of the work has been on lipids containing at least one or two water molecules per lipid molecule.

When in contact with water (or water vapor), phospholipids incorporate a limited amount of water and swell to form bilayers separated by water layers (see figure-1.2). The extent of this swelling depends on the specific lipid under consideration. In general the swelling is more if the head-group is charged. If more water is present in the system than what can be taken up by the lipid, there is a coexistence of the lamellar

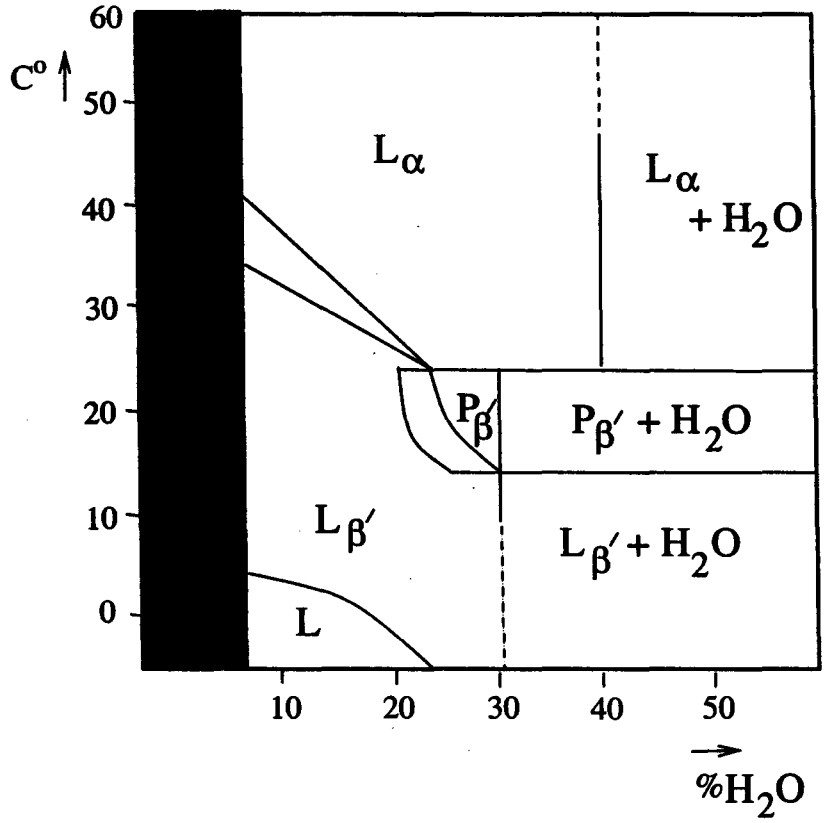

Figure 1.3: **Experimental phase diagram of DMPC.** (From ref. [4])

mesophase and water. As the concentration of water or the temperature is varied, there can be phase transitions among the lamellar phases. A typical phase diagram is shown in figure-1.3 [4].

In the high temperature L_α phase, the chains have a liquid like order (figure-1.4). The name L_α originates from the fact that the liquid like conformation of the chains is called the α-conformation and the (quasi) long range one-dimensional lamellar organization of the lipid molecules is denoted by the letter L. The x-ray diffraction pattern from these chains is characterized by a broad and diffuse band at around 4.6 Å, very similar to the band observed in liquid paraffins [5]. In biophysics literature this phase is often referred to as the liquid crystalline phase.

The calorimetric studies of Chapman et. al. in 1967 [6] revealed that hydrated samples of lipids undergo a strongly first order chain ordering transition (called the

main-transition) in which the chains go from the α configuration to an all-*trans* conformation. This phase is called the $L_{\beta'}$ or gel phase (figure-1.4). The area per chain is lower and the bilayer thickness is higher in this phase than in the L_α phase. The chains become stretched and rigid (though they may still have some rotational degree of freedom [5]) and also acquire some degree of positional order in the plane of the bilayer, though it is not clear whether this ordering is hexatic or 2-D crystalline. Experiments show that the in-plane positional order is correlated over distances of $\approx$1000 Å [7] and hence the term 'chain-lattice' is often used to refer to the chain ordering. The x-ray pattern from these chains show typically one or two strong sharp reflections at $\approx$4.2 Å. Such an arrangement of the chains is referred to as the β arrangement if the chains are parallel to the bilayer normal and as the β' arrangement if the chains are tilted with respect to the layer normal. In some cases, the chains of the opposite monolayers of the bilayer may inter-digitate. This is denoted by the letter I. Though in the L_β, $L_{\beta'}$ and L_{β_I} phases the chains are ordered on a lattice, the head-groups are still disordered. Figure 1.5-A illustrates this situation.

In some phospholipids at high humidity, just below the main-transition, the lipid bilayers are no longer flat but have a one dimensional periodic height modulation (see figure-1.6). The x-ray diffraction pattern from this phase can be indexed on a two dimensional oblique lattice. This phase is called the $P_{\beta'}$ phase (the β' indicates that the chains are ordered and tilted and the P indicates a two-dimensional lattice). Because of it's corrugated ripple like structure, this phase is also called the ripple phase. The $P_{\beta'}$ -$L_{\beta'}$ transition is often called the pre-transition.

Transition to yet another phase was discovered in DPPC stored at low temperatures for a few days [8]. This transition, which is again first order occurs at a temperature below the pre-transition temperature and is referred to as the sub-transition. At the sub-transition, the head-groups also get ordered and the lipid goes to a highly ordered (but not yet a fully three dimensional crystalline [9]) state called the $L_{c'}$ phase. The

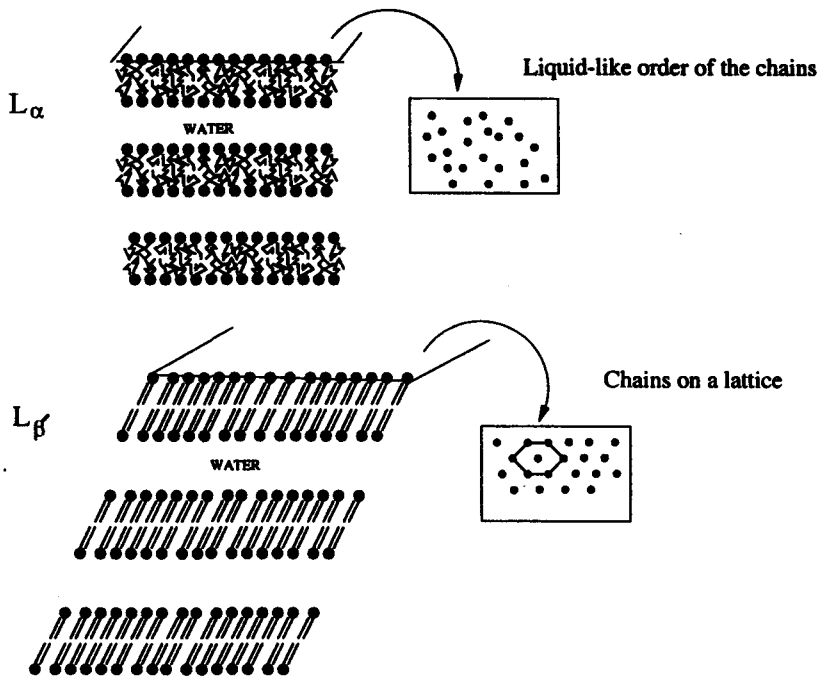

Figure 1.4: **Schematic diagram of the structure of L_α and $L_{\beta'}$ phases.**

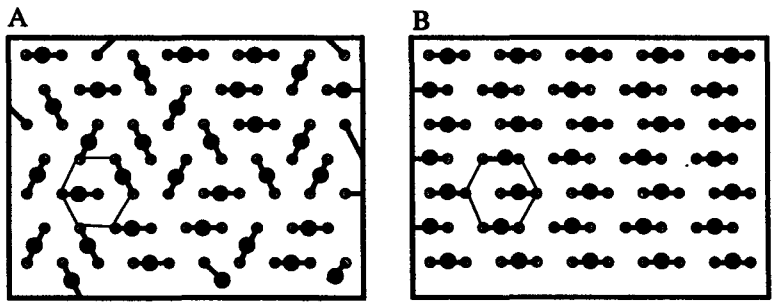

'igure 1.5: **The small dots represent the chains that are arranged on a riangular lattice. The bigger dots represent the head-groups that are isordered in the $L_{\beta'}$ phase (A) but get ordered in the $L_{C'}$ phase (B).**

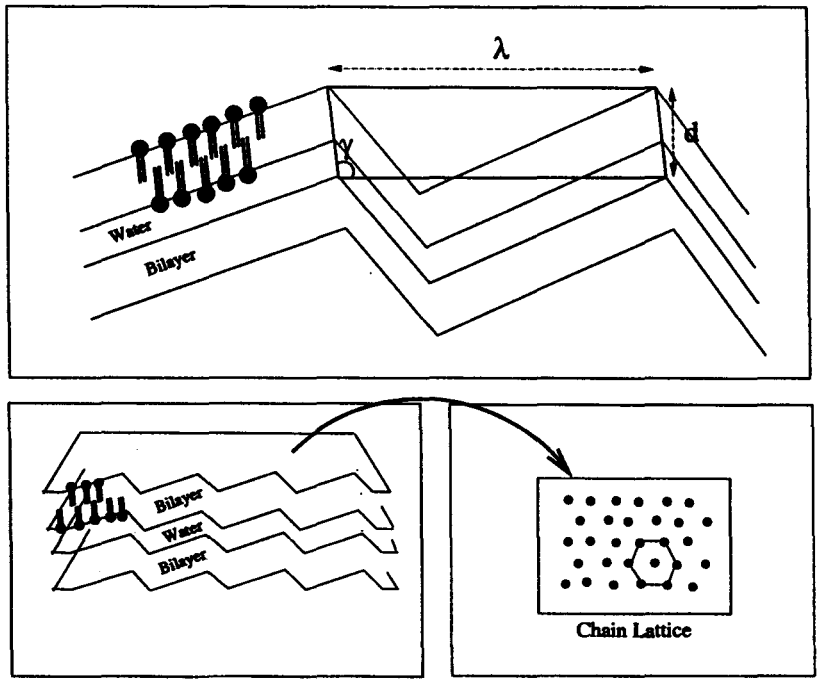

Figure 1.6: **Schematic diagram of the structure of the ripple ($P_{\beta'}$) phase.**

transition from the $L_{\beta'}$ to the $L_{c'}$ phase is like an order-disorder transition (of dimers on a lattice [10]) where the head-groups get ordered into a super-lattice without disturbing the underlying chain lattice. Figure-1.5 explains the structural changes that take place at this transition.

A typical DSC (differential scanning calorimetry) curve showing all the transitions discussed above is shown in figure-1.7. The latent heat for the L_{α} to $P_{\beta'}$ main-transition is large whereas the latent heat for the $P_{\beta'}$ to $L_{\beta'}$ pre-transition is about $\frac{1}{10}$ that of the main-transition. The latent heat for the sub-transition is also less than that of the main-transition.

Recent experiments revealed that the $L_{\beta'}$ phase is actually composed of three distinct phases [7]. These phases differ from each other in the direction of the tilt of the chains with respect to the lattice. In the $L_{\beta'_F}$ phase, the chains tilt towards the nearest-neighbor, in the $L_{\beta'_I}$ phase they tilt towards the next-nearest-neighbor and in the $L_{\beta'_L}$ phase, they have an intermediate tilt. Figure-1.8 gives the recent phase-

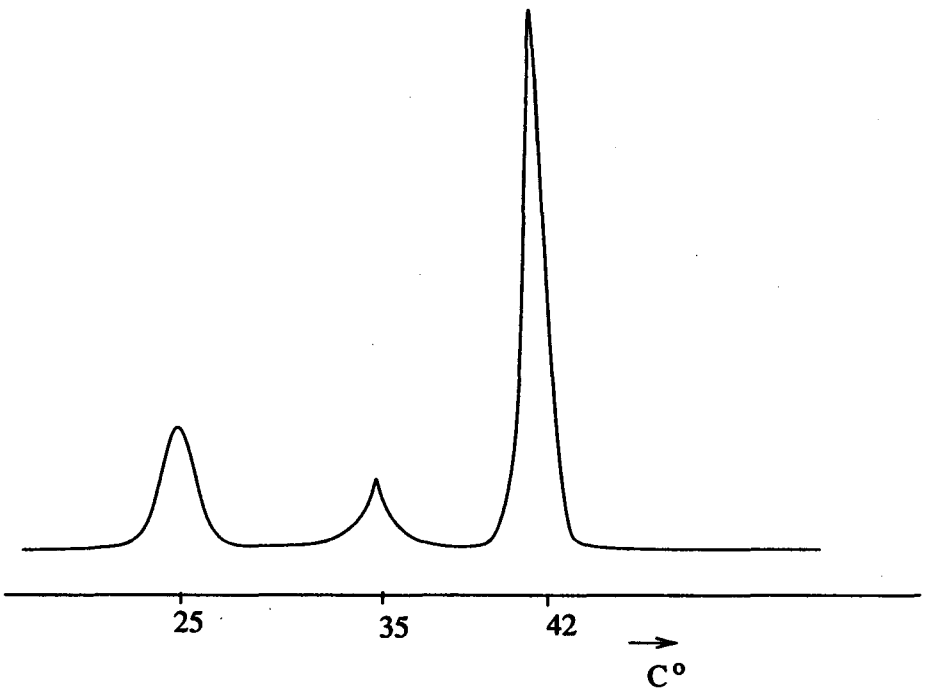

Figure 1.7: **A typical DSC curve for PCs in excess water.** The temperature here correspond to the transition temperatures of DPPC [3].

diagram of DMPC bilayers and figure-1.9 illustrates the structure of each of the three $L_{\beta'}$ phases.

1.1.4 Chain tilt verses interdigitation

The size of the head-group generally dictates whether or not the chains are tilted or interdigitated in the gel phase. In lipids like DPPE, where the head-group is relatively small, the stiff all-*trans* chains are parallel to the layer normal and do not tilt. The distance between nearest neighbors in this case is dictated by the chain-chain van der Waals interactions. As the head group size is increased the chains are forced to be further apart than their ideal separation. By tilting, the chains can reduce the perpendicular distance between the nearest neighbors thus maximizing the van der Waals interaction, and at the same time accommodate the large head-groups. This dependence of tilt on head-group size has in fact been observed experimentally. In one experiment, methyl groups were added one at a time to DPPE (with no tilt in the gel phase) till DPPE was converted to DPPC with a bulky head and a tilt of

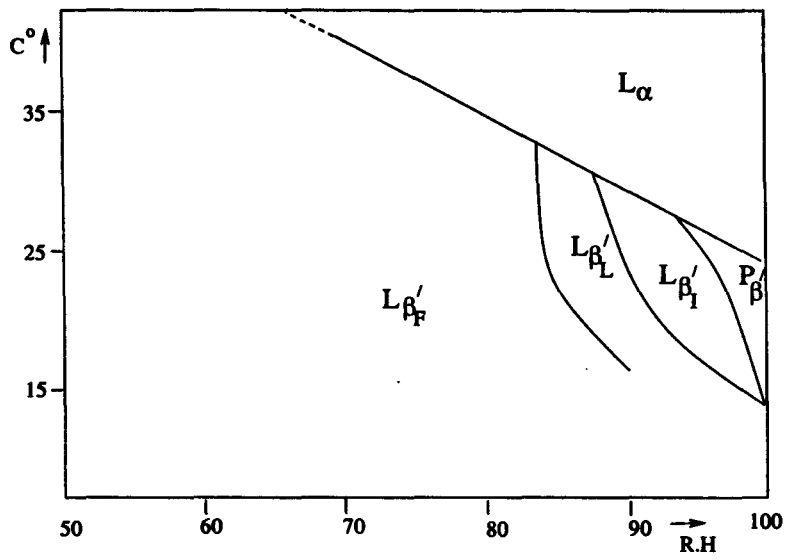

Figure 1.8: **Recent phase diagram (schematic) of DMPC (ref. [7]).** The structures of the three $L_{\beta'}$ phases are given in figure 1.9.

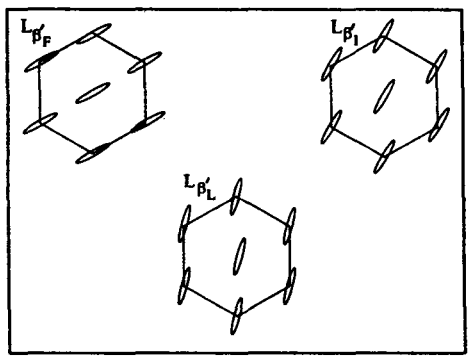

Figure 1.9: **Schematic diagram of the structure of the three $L_{\beta'}$ phases.**

about 30° in the gel phase [11]. In another set of experiments, the effective head-group size was increased by changing the pH of the environment and thus imparting a charge to the head-groups. Again the chains were observed to go from a non-tilted to tilted state in the gel phase as head size was increased [12].

It is believed that the tilt of the chains is a result of parallel shifting up (or down) of adjacent chains by one zigzag unit of the stiff all-*trans* chain, that is, by about 2.5 Å. The chain lattice typically has a lattice parameter of ≈4 Å. This implies a tilt of about 30° for the chains, this value agrees very well with the observed value of the tilt in the $L_{\beta'}$ phase.

If the head-group is very big, the tilting mechanism is not sufficient to achieve the ideal chain packing. In this case the chains may interdigitate to form a closed packed structure. The mechanism that decides whether a tilted structure is preferred or an interdigitated one, is rather subtle and poorly understood. Small differences in the head-group or the linkage group can make the gel phase go from a tilted-chain to an interdigitated-chain structure. For example, the naturally occurring DPPC that we have been discussing so far has the head attached to one side of the backbone (3 position) and the chains are at 1 and 2 position (see figure-1.1). This compound, called 1,2 C_{16}PC, has a tilted $L_{\beta'}$ phase and a $P_{\beta'}$ phase. But it is possible to synthesize 1,3 C_{16}PC where the head is attached to the middle carbon. In this case the chains interdigitate in the gel phase and the compound does not exhibit a $P_{\beta'}$ phase [3]. Similarly, changing the ester linkage of DPPC (without disturbing the head-group or the chain region) to an ether linkage gives DHPC, which again has an interdigitated L_{β_I} phase but exhibits a $P_{\beta'}$ at higher temperature and humidity [13].

1.2 The ripple ($P_{\beta'}$) phase

The ripple phase has been a subject of almost constant experimental and theoretical activity ever since its discovery by Tardieu et. al. in 1973 [5]. The difficulty

in studying this phase stems from the fact that it has a modulated structure at a length scale intermediate between the molecular and the macroscopic. Although this phase may never occur in a biologically relevant situation, it nevertheless provides interesting opportunities to study fundamental competing lipid interactions and their influence on the bilayer shape.

The equilibrium structure of the ripple phase has been extensively studied using diffraction (x-ray [4, 5, 14, 15, 16, 17] and neutron scattering [18]) and freeze fracture (electron microscopy [19, 20, 21, 22, 23, 24] and scanning tunneling microscopy [25]) techniques. The freeze-fracture technique was developed by Steere in 1957 [26]. The basic idea is to fix the structure of a liquid/soft material by sudden cooling and then to obtain a copy of the structure by deposition of a suitable material (usually a metal) on the surface of the sample. The copy is then studied using transmission electron microscopy (TEM). A thin layer of the sample is trapped between two plates, quickly frozen (by for example dipping in liquid freon) and then fractured under vacuum. The fractured surface is replicated by evaporating a thin metal (platinum) layer at an angle to the fractured surface; the metal film is followed by a thicker carbon layer for strength. The original sample is cleaned off and the replica is then examined by TEM. The lateral resolution of the TEM images is limited by the size of the metal film grains to about 2 nm. Image analysis can improve the resolution especially for periodic surfaces [24, 25]. Vertical steps in the fractured surface as small as 0.5 nm can be detected because of shadowing effects of the oblique metal deposition.

The ripple phase has been seen in phosphatidylcholines (PCs), phosphatidylglycerols (PGs) and phosphatidic acids (PAs). Most of the studies have been in 1,2 PCs. Various experiments have indicated the existence of two types of ripple phases: the stable asymmetric phase and the metastable symmetric phase. We describe these phases below.

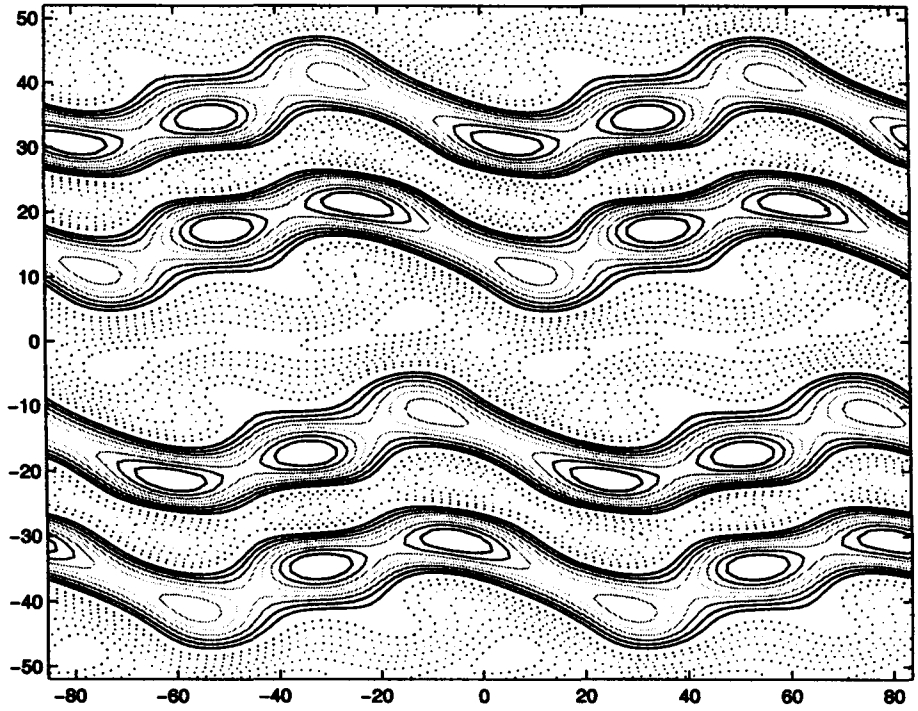

Figure 1.10: **Electron density map of DLPC at -7°C and 77% by weight of water, calculated using the phases given in ref. [5].**

1.2.1 Stable asymmetric ripples

The common type of ripples detected in x-ray experiments have an oblique unit cell. The word asymmetric (symmetric) is used to indicate the absence (presence) of a plane of reflection perpendicular to the ripple wave-vector. Though the ripple phase of phospholipids had been first observed by freeze fracture electron microscopy techniques [19, 20, 21], the first systematic study of this phase was by Tardieu et. al. in 1973 [5]. The x-ray diffraction pattern from DLPC (in water and at a temperature of -7°C and a concentration of 77% by weight of water) was phased by a 'pattern recognition' technique (to be discussed in chapter II) and the electron density map was calculated (see figure-1.10).

In the electron density map of Tardieu et. al., the bilayers are height modulated and have a smooth but asymmetric shape. The structure corresponds to a 2-D oblique unit cell (oblique plane group p2); the ripple wavelength (λ_r) is 85.3 Å, the lamellar periodicity (d) is 55.3 Å and the angle $\gamma = 110^o$. From the electron density map, the peak-to-peak amplitude is seen to be about 15 Å and the bilayer thickness about

35 Å. On the basis of the electron density maps, Tardieu et. al. propose a structure of the ripple phase where the chains are pictured to be stiff (in the β' configuration), with a constant tilt with respect to the normal to the average bilayer plane along the rippling direction; the height modulation arises from the fact that each chain is relatively shifted with respect to their neighbors along its long axis. Though this picture is probably very close to the real structure, the authors themselves point out that the experimental evidence presented in their paper is not enough to rule out other possibilities.

λ_r, d and γ are the crystallographic parameters of the ripples which can be read off directly from the x-ray diffraction pattern of oriented samples and are therefore well known. λ_r=150 Å, d= 55.3 Å and $\gamma = 100^o$ are typical values for ripples in DMPC [4, 5, 14]. The wide angle reflections from the chains in the $P_{\beta'}$ phase are too broad to be interpreted unambiguously. Inspite of that there are indications [4] that the chains are stretched, tilted and are packed in a hexagonal lattice. This lattice goes to a distorted hexagonal or centered rectangular lattice at the $P_{\beta'}$ to $L_{\beta'}$ transition.

In PCs, the ripple parameters do not change appreciably with temperature [4, 27] though they do depend on the humidity [4, 14]. The bilayer repeat distance (d) increases almost linearly and the angle γ decreases with increasing water concentration (ϕ_w). With increasing ϕ_w, the ripple wavelength (λ_r) decreases slightly and then saturates. At similar ϕ_w values, as the chain length increases, both d and λ_r increase. γ does not have any clear-cut dependence on the chain length [14].

Both the main and the pre-transition temperatures systematically increase with the number of carbon atoms(N_C) in the chains but the increase is more rapid for the pre-transition with the result that the temperature range of existence of the $P_{\beta'}$ phase decreases with increasing chain length till above $N_C = 22$ the $P_{\beta'}$ phase disappears all together. The latent heat of the main-transition has a linear dependence on the

chain length but the latent heat of the pre-transition is independent of the chain length. This may indicate that the pre-transition is associated with some interfacial or surface property of the lipids [14]. Recent studies [17] have shown that the temperature range of the ripple phase is larger in mixed chain lipids (where one chain is longer than the other) than in the homo-chained derivatives of the same molecular weight. The latent heat associated with the pre-transition in mixed-chain lipids is rather small and for this reason the pre-transition was undetected in such lipids for a long time [29]. Lipids with unsaturated chains have a smaller range of $P_{\beta'}$ phase than the saturated chain lipids. Pre-transition has not been detected for lipids with chains in 1,3 positions: these isomers probably do not have a $P_{\beta'}$ phase.

Extensive x-ray and DSC studies have been done by the group of Cevc [28] on phospholipid bilayers. Phosphatidylglycerols and dimethylphosphatidylethanolamine (apart from the phosphatidylcholines) are reported to form the ripple phase. Head group effects have been studied by looking at mixtures of lipids with different heads and also by looking at the effect of pH and ion binding. From the results of these experiments, empirical expressions are proposed that can predict the sub, pre and main-transition temperatures. These expressions have the general form : $T_{tr} = a + \frac{b}{N_c} + cN_c^2$ where N_c is the chain length and the constants are presumably determined by the specific head-group interactions. Though it is interesting that these transition temperatures can all be written in the same general form, these empirical formulae do not in any way indicate the real mechanism of ripple formation. From these and other studies [3], it is widely believed that the head-chain size mismatch, tilting and rippling are interconnected [29, 28] and that head-group hydration and chain packing play important roles in the formation of ripples, but the reason why a rippled structure is preferred over a tilted-chain structure is still obscure.

The best theory so far (in terms of internal consistency and agreement with experiments) for the ripple phase is perhaps that of Chen et. al. [30] (see chapter V for

a detailed discussion). They proposed a Landau theory for the ripple phase where a coupling of the divergence in the chain tilt to the layer curvature leads to a height modulation. A clear prediction of this theory is that only symmetric ripples are possible in an achiral system. In view of this, Katsaras and Raghunathan [31] conducted x-ray diffraction experiments on chiral and racemic DMPC and showed that the diffraction patterns from the two samples were very similar: in particular, both correspond to an oblique unit cell indicating that the ripples are asymmetric. This can still be reconciled with the predictions of ref. [30] if there is a separation of the two enantiomers in the racemic mixture, but later studies [32] have ruled out this possibility.

Janiak et. al. [4] discuss the possibility of the ripple phase being due to thickness modulations rather than height modulations of the bilayers. They construct a model for the two possible structures and calculate the expected pattern from each model. This is then compared to the observed intensities. The crystallographic R value is calculated in each case ($R = \frac{\sum||F_o|-|F_c||}{\sum|F_c|}$, where F_o and F_c are the observed and calculated structure factors, respectively). It was found that the R value for a height modulated model (assumed to be sinusoidal) is much lower than that for a thickness modulated one. Thus Janiak et. al. unambiguously proved that the ripple phase is a height modulated phase. The peak-to-peak amplitude of the ripples was estimated to be about 15 Å .

From the analysis of the projected electron density on the average bilayer plane, Wack and Webb [14] argue that the ripples have a saw-tooth shape. They also argue that the chain length dependence of the lipid bilayer thickness (discussed earlier) rules out models of the ripple phase where substantial fraction (> 10 %) of the chains are molten.

Sun et. al. [16] employed a modeling and fitting technique (reviewed in the next

chapter) to phase the DMPC data of Wack and Webb [14]. In the electron density map reported in ref. [16], the ripples show a saw-tooth shaped profile with the major arm of the saw-tooth being about twice as long as the minor arm. The bilayer thickness and the electron density in head-group region of the major arm is found to be larger than that of the minor arm. The value of the bilayer thickness in the major arm is comparable to the thickness of DMPC bilayers in the $L_{\beta'}$ phase whereas the thickness in the minor arm is comparable to that in the L_{α} phase. This lead Sun et. al. to hypothesize that the major arm of the ripple is in the $L_{\beta'}$ phase whereas the minor arm is in the L_{α} phase. This microphase separation picture is inconsistent with other experiments (this will be discussed in detail in chapter III).

Scanning tunneling microscopy (STM) techniques have recently been used to look at freeze-fractured samples of lipids in the ripple phase [25]. Special care has to be taken to prepare samples for STM studies. The samples have to be stiffened (by deposition of silver in addition to the platinum and carbon mentioned before) and have to be examined in moisture free conditions for the results of STM to be reliable. The group of Zasadzinski has combined image processing and STM techniques to get structural details of the ripple phase hitherto not measurable by freeze-fracture methods. Using this technique, the asymmetric shape obtained by x-ray studies [5, 16] has been confirmed, though in these studies, the Fourier expansion of the shape yields only the first two harmonics, contrary to the results of x-ray studies (see chapter III for detailed discussions). At 23°C for DMPC, it is found that λ_r=107±10 Å and the peak-to-peak amplitude of the ripples, A=24 Å. At 20°C, these values are λ_r=106±10 Å, A_r= 11 Å.

Hentschel and Rustichelli [33] report x-ray diffraction experiments on highly aligned DMPC bilayers where λ_r and d were found to be similar to above values but γ was found to be 90°. These results are contrary to all other reports on the ripple phase. This contradiction might be due to the specific method of sample preparation that is very different from those used by other experimentalists. Another possibility is that

the reflections from the coexisting $L_{\beta'}$ phase[1] interferes with correct interpretation of the diffraction pattern. They estimated the tilt of the chains to be 26° with respect to the average layer normal. With respect to the chain lattice, the chains tilt towards their nearest neighbors; this situation is same as in the $L_{\beta'_F}$ phase of ref. [7]. It is argued by Hentschel and Rustichelli that the rippling direction is perpendicular this chain tilt direction. These results may not be correct in view of the coexistence of the $L_{\beta'}$ phase.

1.2.2 Metastable symmetric ripples

In many freeze fracture studies [19, 20, 21, 22, 23, 24] of the ripple phase, along with the asymmetric ripples discussed above, ripples with a larger periodicity (about 1.8 times that of the coexisting asymmetric ripples) are also seen (see figure 1.11). In x-ray studies, these ripples are characterized by a 2-D rectangular unit cell and are called symmetric ripples. These ripples are referred to as Λ-ripples in freeze fracture literature. In x-ray experiments [15, 34, 35, 36] the Λ-ripples show up as fainter reflection (for this reason they are also called secondary ripples) corresponding to modulations where γ is 90° and wavelength is about 1.8 times that of the coexisting asymmetric ripples. These Λ-ripples are metastable and appear only on cooling the sample from the L_α phase and not while heating from the $L_{\beta'}$ phase [37].

By careful analysis of the height profile of the Λ-ripple profiles, it has been shown that these have a groove at the top thus giving them a non-centrosymmetric "M"-shape [22, 24] (see figure 1.11C). Each repeating "M"-shaped unit of the symmetric ripple can be pictured as two one-wavelength-long units of the asymmetric ripples joined with one of the units rotated by 180°; such a structure has the configuration "major arm-minor arm-minor arm-major arm" with the minor arms joining up to form the groove at the top.

[1] it is clear from the photograph of the diffraction pattern presented in ref. [33] that in these experiments there is a coexistence of the $L_{\beta'}$ and $P_{\beta'}$ phases.

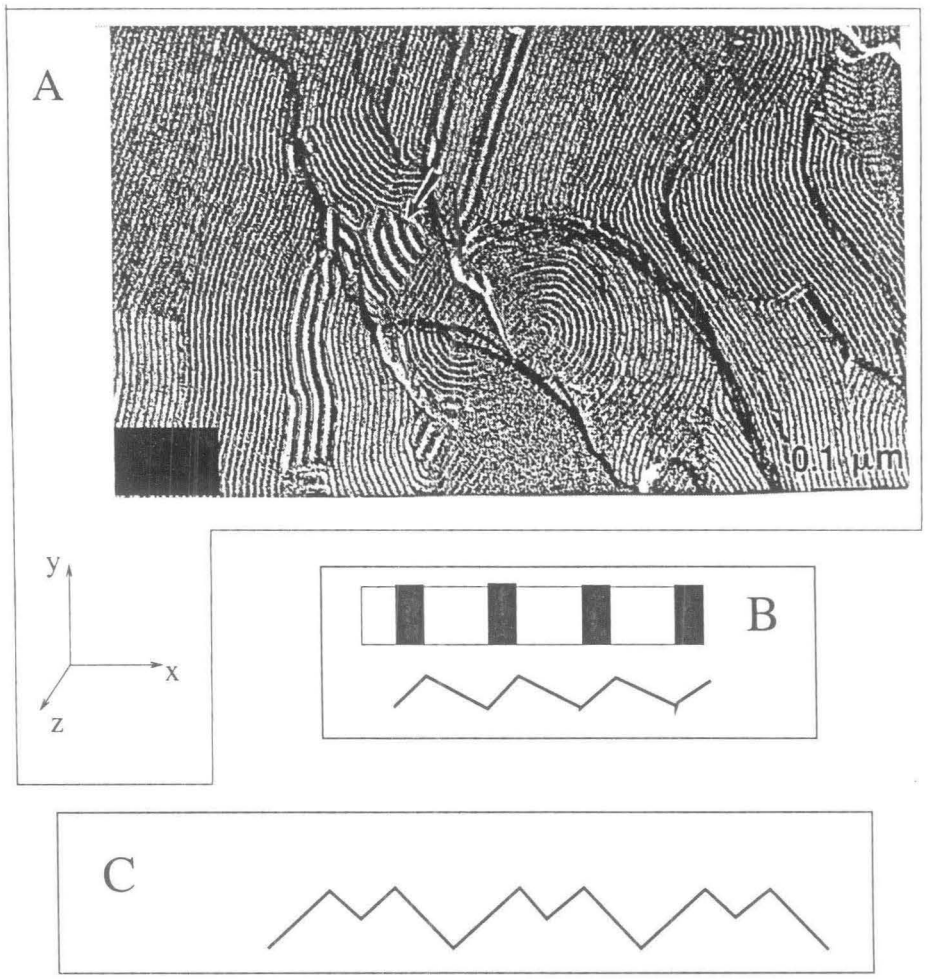

Figure 1.11: **(A): A typical Freeze Fracture micrograph of the ripple phase (DPPC).** A small patch of Λ ripples is indicated by an arrow. (from ref. [24]). The height modulation direction is in the plane of the paper. **(B):** The black and white bands in the figure correspond to the two arms of the saw-tooth-like (or triangular-like) ripples. **(C):** The non-centrosymmetric "M"-shape for the Λ ripples predicted by freeze fracture.

Yao et. al. [15] and Matuoka et. al. [34] have studied the metastable ripples of DPPC using x-ray diffraction methods. In these experiments they report a coexistence of the stable asymmetric ripple with wavelength of $\approx$150 Å and the metastable Λ-ripples. They report a wavelength of about 265 Å, bilayer separation of about 80 Å and $\gamma = 90^o$ for the Λ-ripples. They also show that the Λ-ripples occur only in lipids with number of carbon atoms per chain $\geq$ 13. The structure of the Λ-ripple phase is difficult to probe by x-ray diffraction techniques because the stable and metastable forms coexist and in an unoriented sample, even correct indexing

becomes difficult.

1.2.3 Other studies on the ripple phase

A lot of work has been done on the influence of different chemicals on the ripple phase. The most important of these are the studies on the influence of cholesterol on phosphatidylcholine bilayers [38]. It is hoped that these studies would help in understanding the basic mechanism of lipid-cholesterol interactions, which are of importance in bio-membranes.

Effect of salts particularly divalent cations like Ca^{++} [39] on lipid bilayers has received special attention because these ions get adsorbed on the bilayer surface and introduce a Coulomb repulsion between the layers, thus giving a mechanism by which inter bilayer interactions can be controlled.

A number of spectroscopic techniques have been used to probe the dynamics of the ripple phase [40]. Because of the complex interactions in these systems, the spectroscopic data are very difficult to interpret and contradictions abound in literature.

Other miscellaneous experiments on the ripple phase have been reported; for example experiments on the influence of pressure on the pre-transition [41] and experiments on kinetics of the $P_{\beta'}$ -$L_{\beta'}$ transition [42, 43]. In the absence of any understanding of the microscopic mechanism of ripple formation, it is difficult to unify the results of all these experiments within one framework.

Bibliography

[1] *See for example*, J. R. Holum, Fundamentals of general, organic and biological chemistry. John Wiley and sons, New York 1978.

[2] *See for example*, J. Israelachvili, Intermolecular & Surface Forces, Academic Press, London, 1991.

[3] D. M. Small, Handbook of Lipid Research: The Physical Chemistry of Lipids From Alkanes to Phospholipids. Plenum Press, New York, 1986.

[4] M. J. Janiak, D. M. Small, and G. G. Shipley, Biochemistry **15**, 4575 (1976). M. J. Janiak, D. M. Small, and G. G. Shipley, J. Biol. Chem. **254**, 6068 (1979).

[5] A. Tardieu, V. Luzzati, and F. C. Reman, J. Mol. Biol. **75**, 711 (1973).

[6] D. Chapman, R. M. Williams and D. D. Landbrooke, Chem. Phys. of Lipids, **1**, 455 (1959).

[7] G.S. Smith, E.B. Sirota, C.R. Safinya, and N.A. Clark, Phys. Rev. Lett. **60**, 813 (1988).

[8] S. C. Chen, J. M. Sturtevant and B. J. Gaffney, Proc. Natl. Acad. Sci. U.S.A. **77**, 5060 (1980).

[9] V. A. Raghunathan and J. Katsaras, Phys. Rev. Lett. **74**, 4456 (1995).

[10] J. F. Nagle, C. S. O. Yoloi and S. M. Bhattacharjee, Dimer Models on anisotropic lattices, Phase Transition and Critical Phenomena **13**, C. Domb and J. L. Lebowitz (ed.), Academic Press Great Britain 1989.

[11] D. J. Vaughan and K. M. Keough, FEBS lett. **47**, 158 (1974).

[12] F. Jahnig, K. Harlos, H. Vogel and H. Eibl, Biochemistry **18**, 1459 (1979).
A. Watts, K. Harlos and D. Marsh, Biochim. Biophys. Acta **645**, 91 (1981).

[13] K. Lohner, A. Schuster, G. Degovics, K. Muller and P. Laggner, Chem. Phys. Lipids **44**, 61 (1987).

[14] D. C. Wack and W. W. Webb, Phys. Rev. lett., **61**, 1210 (1988).
D. C. Wack and W. W. Webb, Phys. Rev. A **40**, 2712 (1989).

[15] H. Yao, S. Matuoka, B. Tenchov, and I. Hatta, Biophys. J. **59**, 252 (1991).

[16] W.-J. Sun, S. Tristram-Nagle, R. M. Suter, and J. F. Nagle, Proc. Natl. Acad. Sci. USA **93**, 7008 (1996).

[17] B. A. Cunningham, A. Brown, D. H. Wolfe, W. P. Williams and A. Brain, Phys. Rev. E, **58**, 3662 (1998).

[18] K. Mortrnsen, W. Pfeiffer, E. Sackmann and W. Knoll, Biochim. Biophys. Acta, **945** 221 (1988).
J. Bradshaw, M. Edenborough, P. Sizer and A. Watts, Biochim. Biophys. Acta **987**, 111 (1989).

[19] P. Pinta da Silva, J. Microsc. **12**, 185 (1971).

[20] A. J. Verkleij, P. H. J. Ververgaert, L. L. M. Van Deenen and P. F. Elbers, Biochim. Biophys. Acta **288**, 326 (1972).

[21] P. H. J. Ververgaert, A. J. Verkleij, P. F. Elbers and L. L. M. Van Deenen , Biochim. Biophys. Acta **311**, 320 (1973).

[22] C. Gebhardt, H. Gruler and E. Sackmann, Z. Naturforsch. **32c**, 581 (1977).
D. Ruppel and E. Sackmann, J. Phys. (Paris) **44**, 1025 (1983).

E. Sackmann, D. Ruppel and C. Gebhardt, Liquid Crystals of One - and Two-Dimensional Order, W. Helfrich and G. Heppke (ed.), Springer Series in Chemical Physics 11, Springer-Verlag, 1980.

23] E.J. Luna and H.M. McConnell, Biochim. Biophys. Acta **466**, 381 (1977).
B. R. Copeland and H.M. McConnell, Biochim. Biophys. Acta **599**, 95 (1980).

24] J. A. N. Zasadzinski and M. B. Schneider, J. Phys. (Paris) **48**, 2001 (1987).
J. A. N. Zasadzinski, Biochim. Biophys. Acta, **946** 235 (1988).

25] J. T. Woodward and J. A. Zasadzinski, Phys. Rev. E **53**, R3044 (1996).
J. T. Woodward and J. A. Zasadzinski, Biophys. J. **72**, 964 (1997).

26] R. L. Steere, J. Biophys. Biochim. Cytol. **3**, 45 (1957).

27] Y. Inoko, T. Mitsui, K. Ohki, T. Sekiya, and Y. Nozawa, Phys. Stat. Sol. (a) **61**, 115 (1980).

28] G. Cevc, A. Watts and D. Marsh, Biochemistry **20**, 4955 (1981).
G. Cevc, Biochim. Biophys. Acta **1062**, 59 (1991).

29] J. Stumpel, H. Eibl and A. Nicksch, Biochim. Biophys. Acta **727**, 246 (1983).

30] T. C. Lubensky and F. C. MacKintosh, Phys. Rev. Lett. **71**, 1565 (1993);
C.-M. Chen, T.C. Lubensky, and F.C. MacKintosh, Phys. Rev. E **51**, 504 (1995).

31] J. Katsaras and V. A. Raghunathan, Phys. Rev. Lett. **74**, 2022 (1995).

32] J. Katsaras, R. F. Epand, and R. M. Epand, Phys. Rev. E **55**, 3751 (1997).

33] M.P. Hentschel and F. Rustichelli, Phys. Rev. Lett. **66** 903 (1991).

34] S. Matuoka, H. Yao, S. Kato and I. Hatta, Biophys. J. **64**, 1456 (1993).

35] P. C. Mason, B. D. Gaulin, R. M. Epand, G. D. Wignall and J. S. Lin, Phys. Rev. E **59**, 3361 (1999).

36] M. Rappolt and G. Rapp, Eur. Biophys. J. **24**, 381 (1996).

[37] B. G. Tenchov, H.. Yao and I. Hata, Biophys. J. **56**, 757 (1989).

[38] D. H. Wolfe, L. J. Lis, O. Kucuk, M. P. Westerman, B. A. Cunninggham, S. B. Qadri, W. Bras and P. J. Quinn, Phys. Rev. Lett. **68**, 1085 (1992).
S. Matuoka, S. Kato and I. Hatta, Biophys. J. **67** 728 (1994).

[39] L. J. Lis, W. T. Lis, V. A. Parsegian and R. P. Rand, Biochemistry **20**, 1771 (1981).
A. Watts, K. Harlos, W. Maschke and D. Marsh, Biochim. Biophys. Acta **510**, 63 (1978).

[40] D. Marsh, Biochemistry **19**, 1632 (1980). R. J. Wittebort, C. F. Schmidt and R. G. Griffin, Biochemistry **20**, 4223 (1981).
P. Meier, A. Blume, E. Ohmes, F. Neugebauer and G. Kothe, Biochemistry **21**, 526 (1982).
M. J. Ruocco, A. Makriyannis, D. J. Siminovitch and R. G. Griffin, Biochemistry **24**, 4844 (1985).
W. Wu and L. Chi, Biochim. Biophys. Acta **1026** 225 (1990)

[41] M. Caffrey, J. Hogan and A. Mencke, Biophys. J., **60**, 456 (1991).

[42] G. Rapp, M. Rappolt and P. Laggner, Progr. Colloid Polym. Sci. **93** 25 (1993)

[43] S. Kato and T. Kubo, Chem. Phys. Lipids **90**, 31 (1997).